Magnetic Resonance Letters 2 (2022) 1–8

Contents lists available at ScienceDirect

Magnetic Resonance Letters

journal homepage: www.keaipublishing.com/MRL

Research Article

Second-order phase correction of NMR spectra acquired using linear frequency-sweeps

Dedicated to Professor Xiuwen Han on the occasion of her 80th birthday

Zhehong Gan*, Ivan Hung

National High Magnetic Field Laboratory, 1800 East Paul Dirac Drive, Tallahassee, FL, 32310, USA

ARTICLE INFO

Article history:
Received 16 June 2021
Received in revised form 23 July 2021
Accepted 30 August 2021
Available online 17 September 2021

Keywords:
Second-order phase
Noise
Line shape
Absorptive
Dispersive
Frequency sweep
CHIRP
WURST
Adiabatic
Broadband
CPMG
Spin-echo
Wideline
^{35}Cl

ABSTRACT

NMR spectra acquired with experiments using frequency-sweeps such as the wide-band uniform-rate smooth truncation (WURST) spin-echo and Carr-Purcell-Meiboom-Gill (CPMG) sequences cannot be absorptively phased by using only conventional zeroth- and first-order phase correction. Implementation of phase correction up to the second-order is described for obtaining absorptive spectra, which have more desirable line shapes and noise properties than magnitude spectra. The relationship of the second-order phase to the parameters of frequency sweeps is derived. The second-order phasing in the frequency-domain is equivalent to a point spread in the time-domain signal. The application of second-order phase correction is demonstrated with a wideline ^{35}Cl CPMG spikelet spectrum.

1. Introduction

Fourier-transformation of time-domain nuclear magnetic resonance (NMR) signals yields complex spectra with real and imaginary parts represented by absorptive and dispersive line shapes after spectral phasing [1,2]. Spectral phasing usually consists of a constant zeroth-order term, and a first-order term that is linear in frequency. The zeroth-order phase accounts for all the phase accumulated from *rf* transmission through the console, cables, and probe circuitry to the NMR sample, as well as the reverse path for signal reception and quadrature digital acquisition. A number of the variables are not easy to predict

* Corresponding author. National High Magnetic Field Laboratory, 1800 East Paul Dirac Drive, Tallahassee, FL, 32310, USA.
E-mail address: gan@magnet.fsu.edu (Z. Gan).
Peer review under responsibility of Innovation Academy for Precision Measurement Science and Technology (APM), CAS.

https://doi.org/10.1016/j.mrl.2021.100026

such as the sample and probe tuning, but once the settings are fixed, the zeroth-order phase remains constant, which is an essential requirement for signal averaging and multi-dimensional NMR experiments. The first-order phase accounts for the time delay of data sampling after signal excitation. These delays are unavoidable due to finite pulse lengths, and the dead time required to switch between transmission and reception. Some other small contributions and variations are less predictable, such as the signal delays caused by signal filtration, cable lengths and the probe resonance circuit. Visual adjustment or automatic routines for phase correction in both the zeroth- and the first-order are usually applied to make the real component of spectra absorptive in appearance. It should be noted that the real and imaginary parts of spectra including their noise are related by Hilbert transformation due to the causality principle [3], and the Kramers-Kronig relation between the absorptive and dispersive frequency responses [2,4]. Therefore, the dispersive imaginary part of a phased spectrum is usually discarded without loss of information. For NMR spectra acquired with monochromatic pulses, the zeroth- and first-order corrections are sufficient to process the spectra as described above. As a result, NMR spectrometers and processing software implement spectral phasing only up to first-order.

Second-order phase correction becomes necessary for spectra acquired using linear frequency-sweeps. Field- or frequency-sweeps were the first methods used for NMR observation [5,6]. The use of sweep methods continued throughout the early development of NMR spectroscopy until the introduction of pulsed time-domain Fourier spectroscopy. The two methods are equivalent between the frequency- and time-domains [2,7], but pulsed Fourier NMR spectroscopy is generally more efficient than the slow-passage continuous wave method [8]. The time-domain approach ultimately prevailed with the development of modern multi-dimensional NMR spectroscopy methods [2]. Nevertheless, some of the advantages of frequency sweeps are still being exploited in pulsed NMR today especially for their low *rf* requirement and broadband properties. Frequency-sweep pulses such as CHIRP, WURST (wide-band uniform-rate smooth truncation) [9], Hyperbolic-Secant [10], DFS (double-frequency sweep) [11], and tanh/tan [12–14] have been used for broadband excitation and refocusing [15,16], heteronuclear decoupling [9,17], population manipulation in quadrupolar nuclei [18,19], ultrafast single-scan 2D NMR [20,21], and multiple-echo signal acquisition using the Carr-Purcell-Meiboom-Gill (CPMG) pulse sequence [22]. Early experiments and simulations in solution NMR have shown a quadratic phase dependence in their frequency profiles. It was found that a spin-echo using two frequency-sweep pulses with sweep rates in a 1:2 ratio results in absorptive spectra using conventional zeroth- and first-order phase correction without the necessity for second-order correction [23]. For solids, WURST pulses are increasingly being used for acquisition of wideline NMR spectra [16], and polarization transfer [24,25], in particular with CPMG multiple-echo acquisition [22,26,27]. Fourier transform of the CPMG echo-train signal yields a manifold of spikelets. Such WURST/CPMG spectra contain a quadratic phase term which cannot be corrected with conventional zeroth- and first-order phase correction. Instead, absolute value magnitude spectra are usually taken for spectral presentation and fitting. The resulting spikelet spectra have absorptive profiles representative of the wideline powder patterns, but the individual spikelets are broadened by the dispersive imaginary component. In addition, the magnitude operation yields an offset in the noise floor, and the white noise property is lost. A false impression of reduced noise levels is created in the noise floor regions, while the uncertainty under the peaks due to the noise remains the same. Magnitude spectra are also unable to distinguish positive and negative peaks. In general, it is desirable to obtain absorptive-phased line shapes if second-order phase correction can be applied for spectra acquired using linear frequency-sweeps.

The main purpose of this work is to describe the origin of the quadratic phase term and derive its relation to frequency-sweep parameters in order to facilitate the implementation of second-order phasing in commercial NMR spectrometers and processing software. In the following, the picture of a sweeping *rf* irradiation across a peak frequency is presented to derive the frequency response. For NMR experiments using multiple frequency-sweeps, the second-order phase of the final NMR signal is presented in the framework of coherence transfer pathways [2,28]. The relationship between the frequency-sweep parameters and the second-order phase is derived along with the discrete form for its implementation in data processing. It is shown that in the time-domain the second-order phase operation is a point-spread function. Finally, the second-order phase correction procedure is demonstrated using a wideline ^{35}Cl WURST/CPMG spectrum of a metallocene sample to illustrate the better line shape and noise properties of absorptive-phase spectra.

2. Theory

A pulse with a linearly varied (or swept) irradiation frequency can be described by a constant frequency sweep rate $\frac{d\omega(t)}{dt}$, a frequency ramp $\omega(t)$, or a quadratic *rf* phase $\phi(t)$,

$$\begin{aligned} \frac{d\omega(t)}{dt} &= \omega' \\ \omega(t) &= \omega' t \\ \phi(t) &= \frac{1}{2}\omega' t^2 \end{aligned} \tag{1}$$

Here $\omega' = \Delta\omega/\tau_p$ is the sweep rate of a pulse of duration τ_p through a frequency range $\Delta\omega$. All three descriptions are equivalent and can be used interchangeably for different purposes. The quadratic phase description is simple to implement and most commonly programmed on spectrometers. Whereas the frequency ramp $\omega(t)$ notation is preferred to describe the

crossing between the *rf* and peak frequency, during which most of the *rf* action occurs. The effective flip angle θ induced by the sweep is related to the so-called adiabaticity parameter

$$\alpha = \frac{\omega_1^2}{\omega'} \tag{2}$$

where ω' is the sweep rate and $\omega_1 = -(S + 1/2)\gamma B_1$ is the effective nutation frequency by the *rf* field including the case for the central transition of a half-integer spin *S*. For $\alpha \ll 1$, a rapid crossing with insufficient *rf* field induces only negligible perturbations or a small effective θ. For $\alpha \gg 1$, a slow frequency sweep drags the spin states adiabatically along the effective *rf* field achieving spin state inversion like a π-pulse. In the intermediate regime, the frequency sweep can generate an efficient excitation; most notably an effective $\pi/2$-pulse occurs when $\alpha \sim 0.25$.

Fig. 1 depicts a pulse with a linear frequency sweep through a peak at frequency ω at a time $t_c = \omega/\omega'$. Such a pulse is typically achieved by a quadratic variation of the *rf* phase. The frequency crossing at t_c induces a rotation which transfers coherence from order p_1 to p_2 as illustrated by the coherence transfer pathway diagram. The instantaneous *rf* phase ϕ_c at the moment of the frequency crossing is given by

$$\phi(t_c) = \frac{\omega^2}{2\omega'} \tag{3}$$

The change of coherence order $\Delta p = p_2 - p_1$ contributes a term exp[-i$\Delta p\phi(t_c)$] to the NMR signal [2,28]. During the time periods before and after t_c, free precession (fp) is assumed and it contributes an additional phase factor exp(-iϕ_{fp}) with

$$\phi_{fp} = p_1\left(\frac{\tau_p}{2} + t_c\right)\omega + p_2\left(\frac{\tau_p}{2} - t_c\right)\omega \tag{4}$$

Thus, the total phase of the NMR signal is

$$\begin{aligned} \phi_{total} &= \phi_{fp} + \Delta p\phi(t_c) \\ &= \frac{\omega\tau_p}{2}(p_2 + p_1) - \frac{\omega^2}{2\omega'}(p_2 - p_1) \end{aligned} \tag{5}$$

Considering that the rotation angle θ is independent of peak frequency ω, the frequency sweep can be equivalently described by a broadband rotation with phase ψ at the center of the pulse as shown in Fig. 1. Then, the first term in Eq. (5) which is linear in frequency represents the signal evolution before and after the θ rotation, and can be compensated by a first-order phase correction to take into account the $\tau_p/2$ delays. The second term, $\frac{\omega^2}{2\omega'}(p_2 - p_1)$, is quadratic in frequency and therefore requires a second-order phase correction. The phase contributions to the NMR signal for experiments using multiple frequency sweeps are additive, therefore the overall second-order phase correction is generally given by

$$S \to S \cdot \exp\left(-i\sum_k \frac{\Delta p_k}{2\omega_k'}\omega^2\right) \tag{6}$$

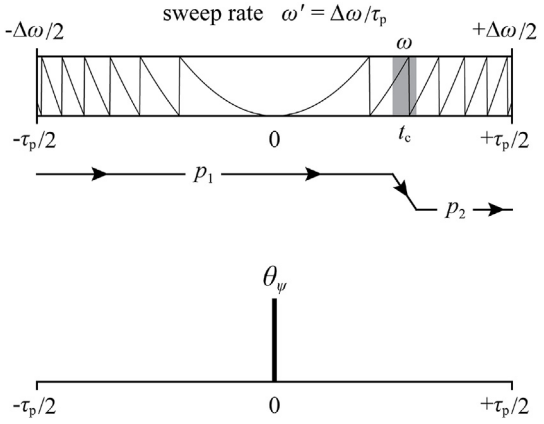

Fig. 1. *rf* frequency sweep of duration τ_p across a peak at frequency ω. The crossing at time $t_c = \omega/\omega'$ (highlighted in grey) induces a rotation θ and coherence transfer from order p_1 to p_2. The frequency sweep can be equivalently described by a broadband rotation at the center and a second-order phase.

The result above was obtained under the assumption of free precession before and after the frequency crossing. However, off-resonance *rf* irradiation during these periods gives rise to a Bloch-Siegert shift [29], which contributes a small quadratic frequency-dependent term that can be corrected by additional second-order phasing. Furthermore, in Eq. (3), the θ rotation and coherence transfer assume a constant *rf* phase during the crossing. However, the *rf* phase is actually changing due to the frequency sweep causing the phase ψ of the θ rotation to lag. The phase lag needs to be taken into account for experiments where the relative phase of the broadband rotation with respect to other pulses is important [27].

Let us first consider a spin-echo using two frequency-swept pulses. If the two frequency sweeps are identical, then for the $p = 0 \rightarrow 1 \rightarrow -1$ coherence transfer pathway the phase of the NMR signal picks up a quadratic term equal to $\exp(i\omega^2/2\omega')$. A second-order phase correction is needed to obtain an absorptive-phase spectrum. However, if the refocusing frequency sweep is twice as fast as that for the excitation pulse (i.e., $\omega'_{rfc} = 2\omega'_{exc}$), then the two quadratic contributions cancel each other since $\Delta p_1 = 1$ and $\Delta p_2 = -2$, and $\frac{\Delta p_1}{2\omega'_{exc}} + \frac{\Delta p_2}{2\omega'_{rfc}} = 0$. Thus, the absorptive spectra can be obtained without requiring second-order phase correction [23]. In more recent applications of frequency sweeps for wideline CPMG experiments, the WURST pulses used for excitation and refocusing are always kept identical. By doing so, the quadratic phase is the same for all CPMG echoes regardless of the coherence transfer pathway and their contributions always add up constructively. Thus, WURST/CPMG spectra acquired in this way contain a quadratic term, and second-order phase correction is necessary to obtain spectra with absorptive line shapes. Frequency sweeps are also often used for polarization inversion and signal enhancement of which the coherence order remains at $p = 0$. Therefore, for these experiments the frequency sweeps do not contribute any second-order phase term because $\Delta p_k = 0$.

3. Results and discussions

Fig. 2 shows the WURST/CPMG pulse sequence, echo signals, and spikelet spectra of a zirconocene dichloride sample [30]. The time-domain echo signals (Fig. 2a) do not show the narrow echoes typical of wideline spectra, but rather 'frequency-dispersed' echoes [16,22]. The spikelet spectrum after zeroth- and first-order phase correction in Fig. 2b shows a remaining term quadratic in frequency. All spikelets become absorptively phased once a second-order phase correction is applied (Fig. 2c). An inverse Fourier transform of the phased spectrum regains the narrow echo signals typical of wideline spectra acquired using monochromatic pulses (Fig. 2d).

It is a common impression that applying frequency-dependent phase correction often causes rolling baselines. This is true for free-induction-decays acquired immediately after excitation. It is unavoidable that a few points at the beginning are either missing or distorted due to transmit/receive switching and dead time, and consequently cause rolling baselines because these points should have high signal intensities. This problem does not occur for full-echo signals, and large first or second-order phasing can be applied without baseline issues. Furthermore, changing the zeroth-order phase only redistributes the absorptive component between the real and imaginary spaces for full-echo signals [31] in contrast to half-echo signals where adjusting the zeroth-order phase mixes the absorptive and dispersive components. This property allows a more precise determination of the zeroth- and first-order phase parameters for full-echo spectra. For CPMG spikelet spectra, individual time-domain echoes determine the profile of the wideline powder pattern. Therefore, the same spectral phase properties described above for full-echoes apply to the powder pattern. However, for individual spikelets, the line shape is determined by the intensities of the echo train, which is actually a half-echo signal. Thus, the spectrum shows a dispersive imaginary component after phasing with a second-order correction (Fig. 2c).

The WURST/CPMG time-domain signals before and after second-order phase correction in Fig. 2 can be described by a point-spread function. Fig. 3 uses simulations of a discrete signal to demonstrate the spread function of second-order phasing. A Fourier transform of a single point signal at $t = 0$ gives a constant spectrum across the spectral window (Fig. 3a and b). After applying a second-order phase to the spectrum (Fig. 3c), its time-domain signal can be obtained with an inverse Fourier transform (Fig. 3d). The simulations show a spread by one point for every 2π or 360° of second-order phase. Both the frequency-domain spectrum (Fig. 3c) and the time-domain signal (Fig. 3d) show a quadratic phase. The spread of time-domain signals requires a larger acquisition window to avoid truncation. Thus, the broadband property of frequency sweeps comes at the expense of not only longer pulses but also larger acquisition windows which reduce the number of CPMG echoes within a finite T_2 relaxation time.

The phase multiplication factor ϕ for the points j = -N/2, -N/2 + 1, …, 0, …N/2−1 in a spectrum is defined by

$$\phi_j = \frac{1}{2}\frac{j^2}{N^2} \cdot phc2 \tag{7}$$

where N is the total number of points. The relationship between the second-order phase correction (*phc2*) and the frequency sweep parameters can be obtained for WURST/CPMG from Eq. (6)

$$phc2 = 4\pi^2 \cdot \frac{SW^2}{\omega'} \tag{8}$$

where SW is the spectral width and ω' is the sweep rate. Noting that for every CPMG echo, $\sum_k \Delta p_k = -1$. If the sweep range $2\pi\Delta\omega$ is equal to SW, then

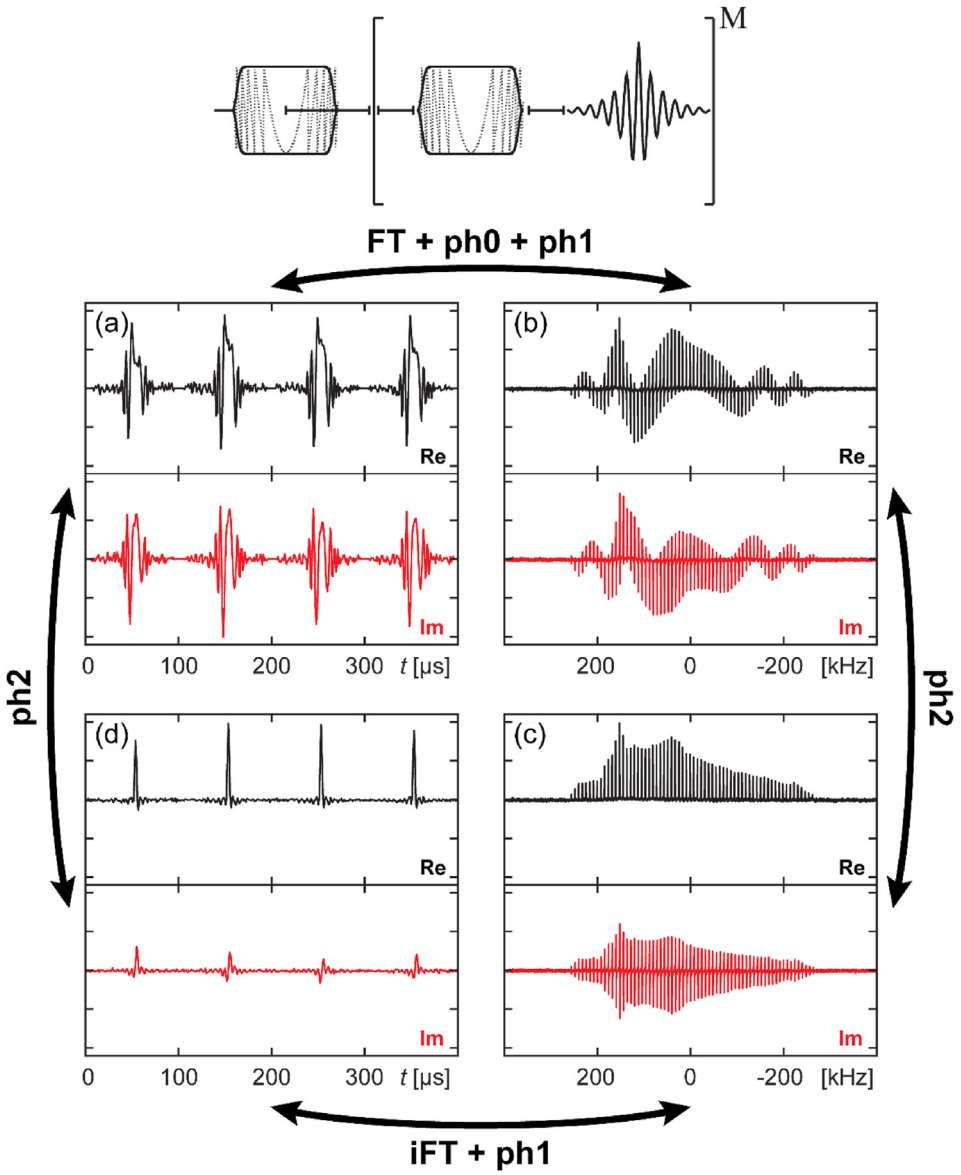

Fig. 2. WURST/CPMG pulse sequence and ^{35}Cl WURST/CPMG (a,d) time-domain echo signals and (b,c) spikelet spectra of static zirconocene dichloride. Spectra obtained with phase correction up to the first- (ph0 and ph1) and second (ph2) orders are shown in (b) and (c), respectively. The signal in (d) obtained after inverse Fourier transformation of (c) illustrates the effect of second-order phasing in the time-domain. Real and imaginary components are shown as black and red traces, respectively. The excitation and refocusing frequency sweeps are kept identical in the WURST/CPMG pulse sequence. The spectrum was acquired at 19.6 T using a Bruker DRX spectrometer and a single-resonance 4 mm MAS probe designed and built at the NHMFL; 50 μs WURST-80 pulses with sweep ranges of 1 MHz and *rf* fields of 17.3 kHz were used; Other parameters were M = 40, spectral width (*SW*) = 1.0 MHz and a recycle delay of 1.0 s.

$$phc2 = 2\pi \cdot \frac{\tau_p}{dw} \tag{9}$$

where *dw* is the dwell time and τ_p is the sweep duration. Eq. (9) shows that the amount of second-order phase correction necessary (in units of 2π) is equal to the duration (in units of the dwell) of a frequency sweep across the whole spectral width. The sign of the phase correction is determined by the direction of the sweep.

Fig. 4a and b compare the noise and line shapes between the phased and magnitude spikelet spectra. In the noise region, the magnitude operation creates a raised floor with reduced noise spread. It is important to note that the uncertainty under the peak regions is largely unchanged. Therefore, the noise level reduction by the magnitude operation is in appearance only. For the phased spectrum, the white noise property is retained across the whole spectral window. As for the line shape, the spikelet profile or the wide line powder pattern are the same between phased and magnitude representations. For individual spikelets, the magnitude spectrum in Fig. 4b shows broader line shape from the dispersive component whereas the phased

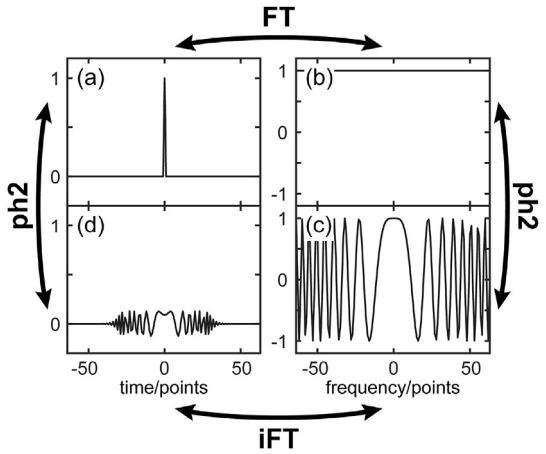

Fig. 3. Simulated (a,d) time-domain echo signals and (b,c) frequency-domain spectra (a,b) without and (c,d) with second-order (ph2) phase. The comparison of (a) and (d) illustrates the point spread from second-order phasing.

spectrum contains the narrow absorptive component only. This is expected because the echo intensity profile which determines the spikelet line shape is equivalent to a half-echo signal. The comparisons show that the real absorptive spectra, here by second-order phase correction, has advantages over the magnitude spectra. If insisting on magnitude representation, taking the absolute value of only the real part (Fig. 4c) would exclude both the noise contribution and the broader dispersive components from the imaginary part as compared with the magnitude operation of the complex spectrum. The inset in Fig. 4c

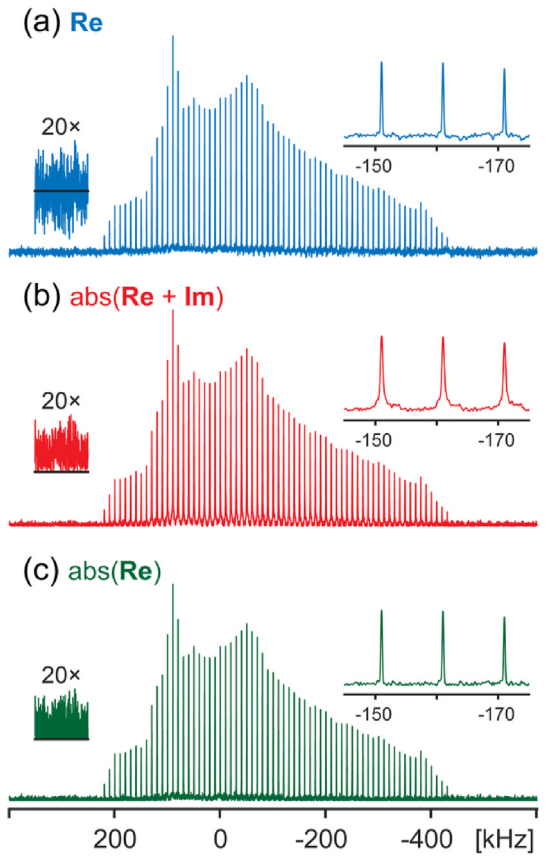

Fig. 4. Comparisons of ^{35}Cl WURST/CPMG spikelet spectra of zirconocene dichloride shown as (a) a real phased spectrum, (b) the magnitude of the real and imaginary components, and (c) the absolute value of the real part after second-order phase correction. The insets show a noise region magnified by a factor of 20, and an expansion of representative spikelet line shapes.

shows the preservation of narrow line shapes for the spikelets. However, this can be achieved only after applying phase correction up to the second order.

4. Conclusion

In summary, we have shown that linear frequency-sweeps can be equivalently described by a broadband rotation and a quadratic phase term. The second-order phase correction can be applied to compensate the quadratic phase term yielding absorptive spectra. The use of second-order phasing is recommended for NMR spectra acquired using frequency-sweeps such as WURST/CPMG for better line shapes and noise properties.

Declaration of interests

The authors declare that they have no known competing financial interests or personal relationships that could have appeared to influence the work reported in this paper.

Acknowledgement

This work was supported by the National High Magnetic Field Laboratory (NHMFL, USA) through NSF DMR-1644779 and the State of Florida.

References

[1] R.R. Ernst, W.A. Anderson, Application of fourier transform spectroscopy to magnetic resonance, Rev. Sci. Instrum. 37 (1) (1966) 93–102, https://doi.org/10.1063/1.1719961.
[2] R.R. Ernst, G. Bodenhausen, A. Wokaun, Principles of Nuclear Magnetic Resonance in One and Two Dimensions, Oxford University Press, New York, 1987.
[3] E. Bartholdi, R.R. Ernst, Fourier spectroscopy and the causality principle, J. Magn. Reson. 11 (1) (1969) 9–19, https://doi.org/10.1016/0022-2364(73)90076-0, 1973.
[4] A. Abragam, The Principles of Nuclear Magnetism, Clarendon Press, 1961.
[5] E.M. Purcell, H.C. Torrey, R.V. Pound, Resonance absorption by nuclear magnetic moments in a solid, Phys. Rev. 69 (1–2) (1946) 37–38, https://doi.org/10.1103/PhysRev.69.37.
[6] F. Bloch, Nuclear Induction. *Phys. Rev.* 70 (7–8) (1946) 460–474, https://doi.org/10.1103/PhysRev.70.460.
[7] I.J. Lowe, R.E. Norberg, Free-induction decays in solids, Phys. Rev. 107 (1) (1957) 46–61, https://doi.org/10.1103/PhysRev.107.46.
[8] R.R. Ernst, Sensitivity enhancement in magnetic resonance, in: J.S. Waugh (Ed.), Advances in Magnetic and Optical Resonance, vol. 2, Academic Press, 1966, pp. 1–135, https://doi.org/10.1016/B978-1-4832-3115-0.50008-9.
[9] E. Kupce, R. Freeman, Adiabatic pulses for wide-band inversion and broad-band decoupling, J. Magn. Reson., Ser. A 115 (2) (1995) 273–276.
[10] M.S. Silver, R.I. Joseph, D.I. Hoult, Highly selective Π2 and π pulse generation, J. Magn. Reson. 59 (2) (1969) 347–351, https://doi.org/10.1016/0022-2364(84)90181-1, 1984.
[11] A.P.M. Kentgens, R. Verhagen, Advantages of double frequency sweeps in static, MAS and MQMAS NMR of spin I=3/2 nuclei, Chem. Phys. Lett. 300 (3–4) (1999) 435–443.
[12] J. Baum, R. Tycko, A. Pines, Broadband and adiabatic inversion of a two-level system by phase-modulated pulses, Phys. Rev. 32 (6) (1985) 3435–3447, https://doi.org/10.1103/PhysRevA.32.3435.
[13] C.J. Hardy, W.A. Edelstein, D. Vatis, Efficient adiabatic fast passage for NMR population inversion in the presence of radiofrequency field inhomogeneity and frequency offsets, J. Magn. Reson. 66 (3) (1969) 470–482, https://doi.org/10.1016/0022-2364(86)90190-3, 1986.
[14] M. Garwood, L. DelaBarre, The return of the frequency sweep: designing adiabatic pulses for contemporary NMR, J. Magn. Reson. 153 (2) (2001) 155–177, https://doi.org/10.1006/jmre.2001.2340.
[15] J.-M. Bohlen, M. Rey, G. Bodenhausen, Refocusing with chirped pulses for broadband excitation without phase dispersion, J. Magn. Reson. 84 (1) (1969) 191–197, https://doi.org/10.1016/0022-2364(89)90018-8, 1989.
[16] R. Bhattacharyya, L. Frydman, Quadrupolar nuclear magnetic resonance spectroscopy in solids using frequency-swept echoing pulses, J. Chem. Phys. 127 (19) (2007) 194503, https://doi.org/10.1063/1.2793783.
[17] E. Kupce, R. Freeman, Stretched adiabatic pulses for broadband spin inversion, J. Magn. Reson., Ser. A 117 (2) (1995) 246–256.
[18] J. Haase, M.S. Conradi, Sensitivity enhancement for NMR of the central transition of quadrupolar nuclei, Chem. Phys. Lett. 209 (3) (1993) 287–291, https://doi.org/10.1016/0009-2614(93)80109-3.
[19] A.P.M. Kentgens, R. Verhagen, Advantages of double frequency sweeps in static, MAS and MQMAS NMR of spin I=3/2 nuclei, Chem. Phys. Lett. 300 (3) (1999) 435–443, https://doi.org/10.1016/S0009-2614(98)01402-X.
[20] Y. Shrot, B. Shapira, L. Frydman, Ultrafast 2D NMR spectroscopy using a continuous spatial encoding of the spin interactions, J. Magn. Reson. 171 (1) (2004) 163–170, https://doi.org/10.1016/j.jmr.2004.08.001.
[21] A. Tal, L. Frydman, Single-scan multidimensional magnetic resonance, Prog. Nucl. Magn. Reson. Spectrosc. 57 (3) (2010) 241–292, https://doi.org/10.1016/j.pnmrs.2010.04.001.
[22] L.A. O'Dell, A.J. Rossini, R.W. Schurko, Acquisition of ultra-wideline NMR spectra from quadrupolar nuclei by frequency stepped WURST-QCPMG, Chem. Phys. Lett. 468 (4–6) (2009) 330–335.
[23] J.M. Bohlen, G. Bodenhausen, Experimental aspects of chirp NMR-spectroscopy, J. Magn. Reson., Ser. A 102 (3) (1993) 293–301.
[24] K.J. Harris, A. Lupulescu, B.E.G. Lucier, L. Frydman, R.W. Schurko, Broadband Adiabatic inversion pulses for cross polarization in wideline solid-state NMR spectroscopy, J. Magn. Reson. 224 (2012) 38–47, https://doi.org/10.1016/j.jmr.2012.08.015.
[25] S. Wi, Z. Gan, R. Schurko, L. Frydman, Cross-polarization phenomena in the NMR of fast spinning solids subject to adiabatic sweeps, J. Chem. Phys. 142 (6) (2015), 064201, https://doi.org/10.1063/1.4907206.
[26] R.W. Schurko, Acquisition of wideline solid-state NMR spectra of quadrupolar nuclei, in: eMagRes, American Cancer Society, 2011, https://doi.org/10.1002/9780470034590.emrstm1199.
[27] I. Hung, Z. Gan, On the practical aspects of recording wideline QCPMG NMR spectra, J. Magn. Reson. 204 (2) (2010) 256–265.
[28] G. Bodenhausen, H. Kogler, R.R. Ernst, Selection of coherence-transfer pathways in NMR pulse experiments, J. Magn. Reson. 58 (3) (1984) 370–388, https://doi.org/10.1016/0022-2364(84)90142-2.
[29] L. Emsley, G. Bodenhausen, Phase shifts induced by transient bloch-siegert effects in NMR, Chem. Phys. Lett. 168 (3) (1990) 297–303, https://doi.org/10.1016/0009-2614(90)85614-I.

[30] A.J. Rossini, R.W. Mills, G.A. Briscoe, E.L. Norton, S.J. Geier, I. Hung, S. Zheng, J. Autschbach, R.W. Schurko, Solid-state chlorine NMR of group IV transition metal organometallic complexes, J. Am. Chem. Soc. 131 (9) (2009) 3317−3330, https://doi.org/10.1021/ja808390a.
[31] I. Hung, P. Gor'kov, Z. Gan, Using the heteronuclear bloch-siegert shift of protons for B1 calibration of insensitive nuclei not present in the sample, J. Magn. Reson. 310 (2020) 106636, https://doi.org/10.1016/j.jmr.2019.106636.

Zhehong Gan obtained his BSc in physics from Zhejiang University in 1984 and PhD in chemical physics from the University of Utah in 1990. He is currently a research professor at the National High Magnetic Field Laboratory in Tallahassee Florida USA. His research interest include NMR methods, theory and applications to solid materials.